Effect of the Characteristics of Nylon Microparticles on Mode-I Interlaminar Fracture Toughness of Carbon-Fibre/Epoxy Composites

Wei-Ting Wang[1], HaNa Yu[2], Kevin Potter[1], Byung Chul Kim[1]*

[1] *Bristol Composites Institute (ACCIS), University of Bristol, Queen's Building, University Walk, Bristol BS8 1TR, UK*

[2] *Department of Mechanical Engineering, University of Bath, Bath, BA2 7AY, UK*

*Corresponding author: B.C.Eric.Kim@bristol.ac.uk

Abstract

Interleaving a laminated composite with thermoplastic particles is known as an effective method to improve the interlaminar fracture toughness. In this work, to provide useful insight into what particle characteristics are the most critical to the toughening effect, the interlaminar fracture behaviours of carbon fibre/epoxy composites interleaved with different types of nylon 6 and 12 particles were investigated in the same range of particle areal weights.

The results showed the particle size affects the toughness only when the particle-matrix interfacial bonding is well established, which is related to the curing temperature relative to the melting temperature of the particle. High interfacial bonding strength allowed the particles to be plastically deformed while bridging the crack, and smaller particles were more effective due to the increased density of particle bridging. It was also found that both the particle size and shape affect thickening of the interlayer, which can cause a knockdown of in-plane laminate properties due to the reduced fibre volume fraction.

Keywords: A. Laminates; B. Fracture toughness; Delamination; D. Mechanical testing

1. Introduction

Despite the many advantages of using high performance fibre reinforced composites for weight critical parts, one of the main concerns is their poor damage tolerance, which can cause large area delamination resulting in a catastrophic failure.

The interlaminar toughness of laminated composites can be improved in many ways. The early studies mainly focused on resin modification; this usually involves incorporation of ductile materials such as elastomers [1,2] or thermoplastics [3-5] with thermoset resin at a molecular level, which provides significant improvement of the fracture toughness of the matrix. However, an effective toughener for bulk resin does not always offer a similar improvement when used within composite laminates, as the interlaminar resin layer thickness is usually too small to fully develop plastic deformation at the crack tip [6]. This localised plastic deformation is an important energy absorption mechanism preventing crack propagation in a bulk polymer. Sela et al. [7] reported that a thicker resin layer can be beneficial to the interlaminar fracture toughness. They also addressed that the 'selective toughening' is useful to reduce stress concentration near the structurally discontinuous locations such as joints in various of composite applications [8].

However, even with any of the aforementioned toughening methods, thermoset matrix based composites generally have a considerably low interlaminar fracture toughness compared to thermoplastic matrix based ones [9], due to the inherent brittleness of the thermosets. Tahir [10] found that carbon fibre/PA12 composite laminates made from commingled yarns exhibited a Mode-I fracture toughness, G_{IC}, of about 3 kJ/m^2, which is about 5-10 times higher than that of typical carbon/epoxy laminates [9].

In order to take the advantage of the ductility of the thermoplastics, methods of interleaving a thermoset based composite laminate with thermoplastic micro-particles began to be used and is known as an effective interlaminar toughening method [5], which not only creates a thicker

resin layer but also includes a ductile secondary material allowing for crack deflection [11]. The inclusion of such particles in a bulk epoxy could cause crack bridging [12] promoting the fracture energy absorption during crack propagation. Such a toughening technique has been patented [13,14] and special prepreg resin systems taking advantage of such a mechanism are commercially available; for example, Hexcel M21 prepreg resin includes polyamide particles (PA6/PA12) as toughenes as well as polyether sulfone (PES) [15].

For bulk polymers, particle bridging is known to be observed when ductile materials are used as particle toughenes. This mechanism allows for stable crack propagation and reduces stress concentration at the crack tip [6,12]. Particle bridging effect requires a good particle-matrix bonding [16]. This adhesion can be achieved by promoting chemical bonding or creating molecular entanglements between the two materials. Nichols *et al*. [17] stressed that the development of the interphase between poly-butylene-terephthalate (PBT) and epoxy molecules is more important than the dispersion of PBT in the epoxy. This molecular entanglement is also referred to as a semi-interpenetrating network (semi-IPN), which can significantly affect the fracture toughness of a modified epoxy resin system [18].

The development of semi-IPN structure requires both material phases in a gel state, which is temperature dependent. Kim *et al.* [18], who studied nylon 6 particles blended in an epoxy at different temperatures, found the morphology of fractured particles changed depending on the mixing temperature. The G_{IC} was improved when the mixing temperature was close to the melting point of nylon 6, but the modulus and yield strength remained unaffected. They also reported the chemical reaction between an amine cured epoxy and nylon 6 particles contributed to the interfacial bonding strength. In contrast, Park *et al*. [19] interleaved a 120°C amine cured carbon/epoxy prepreg laminate with 20 μm nylon 6 particles, and found the G_{IC} was not affected by varying the particle amount. Pairs [15] reported the G_{IC} of M21/T700 composite was nearly doubled by implementing a higher curing temperature than the recommended curing

temperature. Fusion between particles and resin interface was observed, which resulted in a crack shifted from the interlaminar region to the fibre layer [20].

The fabrication of commercial particle toughened prepreg systems involves pre-mixing particles with the liquid resin, followed by a single or double pass impregnation method to create a particle rich surface on the prepreg [21]. In this process, the employed particle amount is inevitably limited due to the increased resin viscosity. Although an interlaminar toughening methods by directly coating the prepreg surface with particles have been reported [19,22,23], their studies on the effect of the particle characteristics on the mechanical performance was rather limited.

This work particularly focuses on the nylon particles as interlaminar toughener, investigating the effect of the particle characteristics of five different types of nylon particles on the interlaminar fracture toughness of carbon/epoxy laminated composites. These particles were made of two types of nylons with different sizes, shapes and surface morphology. The particles were directly deposited on the surface of the prepregs with different areal weights. Their effect on the Mode-I interlaminar fracture toughness and the failure behaviour was experimentally studied. The thickening of the interlaminar resin layer and its potential impact on the fibre volume fraction and the in-plane mechanical property of the toughened laminate were also discussed.

2. Experimental

2.1 Materials

The prepreg material used in this work was HexPly® IM7/8552 (Hexcel, US), which is made of a Poly-ethersulfone (PES) toughened [24] 180°C amine-cured epoxy resin system and intermediate modulus carbon fibres, IM7 (Tohotanex, JP). The 0° and 90° tensile moduli are 164 GPa and 12 GPa [25], respectively.

Five types of nylon particles with different sizes and shapes were used in this work, as listed in Table 1. The material ID was given based on the material type, particle diameter, shape and surface morphology. The number next to the letter 'd' indicates the average particle diameter. The last letter indicates the particle shape and morphology; The PA12-d5s and PA12-d10s have smooth particle surfaces, the PA6-d13r has a higher surface area due to its rough surface, and the PA6-d16a and PA12-d30a have irregular shapes. Nylon 12 has a melting point similar to the recommended curing temperature of the 8552 resin, while the nylon 6's is higher.

2.2 Sample preparation

Nylon particles were dehydrated in a dehumidifier chamber at 80°C for 24 hours before use. Double cantilever beam (DCB) samples, as shown in Figure 1, were made from 30 layers of unidirectional prepregs with dimensions of 340 mm × 120 mm. The nylon particles were uniformly distributed only on the middle interlayer of the laminate (the 15^{th} and 16^{th} plies) by directly spreading the particles on the prepreg surface using a spraying or scraping method. The areal weight was calculated by measuring the weight of the ply before and after the particle deposition. A 12 μm thick PTFE film was inserted between the two layers to create a 50 mm long initial crack.

The curing cycle used in this work was a cycle recommended by the material suppliers; 1 hour dwell at 110°C and 2 hours curing at 180°C. After curing, the panels were cut into coupons with dimensions of approximately 160 mm × 20 mm × 3.7 mm, and hinges were bonded on both sides where the PTFE film was inserted, at the position as required by ASTM D5528 [26]. The side edges of the test coupon were coated with white paint, and grid lines were marked for crack propagation length measurement.

2.3 Measurement of the interlayer thickness

The particle tougheners included in the interlayers resulted in thicker interlayer [27,28]. In order to investigate such thickening effect of different particles, the edges of the double cantilever

beam (DCB) samples were polished and observed using an optical microscopy, as shown in Figure 2. The interlayer thickness was measured using image processing software. Due to the variation of the thickness, the values were averaged from 12 measurements in three photos taken from different locations along the specimen length.

2.4 Measurement of the Mode-I interlaminar fracture toughness

Mode-I fracture toughnesses were measured following ASTM D5528. A universal material testing machine (Shimadzu, JP) with a 1 kN load cell was used at a cross-head speed of 1 mm/min. Each test included two steps; a 3-5 mm long sharp crack tip was formed first by opening the precrack and the specimen was unloaded, and then in the second step, the specimen was reloaded until the crack growth reached about 30 mm from the initial crack tip created in the first step. Crack propagation during test was captured by a video camera (iMETRUM, UK) at a sampling rate of one frame per second. The crack length was manually measured using image analysis software.

The G_{IC} value was calculated using the modified beam theory (MBT) [26], which is described as;

$$G_{IC} = \frac{3P\delta}{2b(a+|\Delta|)} \qquad \text{Equation 1}$$

where P, δ, b, a and Δ are the peak load, cross-head displacement at the peak load, specimen width, crack length and correction factor for the DCB arm, respectively.

2.5 Fractography analysis

To observe the fractured surface and the crack propagation path, the tested DCB samples were cut into a few pieces, as showed in Figure 3. After the longitudinal cut, the cut surface was polished to reveal the side of the crack tip. A scanning electron microscope (TM3030Plus, Hitachi) was used for this observation.

3. Experimental results

3.1 *Toughened layer thickness*

The cross-sectional SEM image showed that in the range of particle areal weight applied to the laminates in this work, the particles were well impregnated with the epoxy resin after curing in the interlayer (Figure 4a). As shown in Figure 4b, the interlayer thickness increased proportionally to the amount of particle at low areal weights (< 20 g/m^2) in general. It was found that the interlayer thickness increase was differently influenced by the average particle size, which can be seen from PA12-d5s, PA12-d10s and PA12-d30a toughened samples in the range of low areal weights (< 20 g/m^2). However, further increase of the particle amount resulted in slightly different trends of thickness change for different particles. The most significant thickening effect was observed when a high areal weight (> 20 g/m^2) of PA6-d13r was applied. Although its particle size was not the greatest among the particles, the interlayer thickness was greater than that of the sample interleaved with PA12-d10s particles with a slightly smaller diameter. This might be resulted from the difference in the particle surface morphology affecting the particle packing behaviour, which is further discussed in Section 4.

3.2 Mode-I DCB test

Most of the nylon 6 and nylon 12 particle-toughened samples exhibited stable crack propagation during the DCB test, as shown in Figure 5. As shown in Figure 5a, the nylon 12 particles were much more effective in toughening than the nylon 6 particles in general. The increase of particle loading contributed to increasing the crack opening load (Figure 5b), while the same trend was not observed in the nylon 6 particle-toughened samples (Figure 5c).

Another difference found from the load-displacement curves was that the nylon 12 particle toughened samples exhibited more ductile response; a rather ‘blunt’ load peak was observed when the crack propagation was initiated (Figure 5a). This became more outstanding as the amount of the particles increased over a certain level. For example, the transition from ‘sharp‘ to ‘blunt’ peak was clear in PA12-d10s, when the particle areal weight increased from

6.25 g/m^2 to 9.66 g/m^2 (Figure 5b). However, this response was not seen in the samples toughened with nylon 6 particles (Figure 5c) where the load drop was rather linear right after reaching the peak load, resulting in no difference from the non-toughened specimens. The different trend of the load-displacement curves between nylon 6 and nylon 12 particles is described in Figure 5d. The particle bridging effect will be further discussed in Section 4.3.

Figure 6a shows the crack growth resistance curve (R-curve) for different toughening particles and all the G_{IC} initiation (G_{IC_init}) values of the tested samples. The increased particle amount resulted in G_{IC} improvement in all the nylon 12 particle-toughened samples, while the small particles (PA12-d5s and PA12-d10s) were more effective than the large particle (PA12-d30a). Although the PA12-d30a particles started being effective when the particle amount was higher than 10 g/m^2, the PA12-d5s and PA12-d10s particles significantly improve the fracture toughness even when it was below 10 g/m^2; the G_{IC} was almost twice that of the non-toughened specimens at 10 g/m^2. This implies that with an areal weight even smaller than 10 g/m^2, the G_{IC_init} of the IM7/8552 composite laminates could become higher than that of composites made with M21 matrix based prepreg (approximately 0.3-0.36 kJ/m^2 [15,20]), which is a commercially available toughened prepreg product produced by the same supplier.

In contrast, the samples interleaved with nylon 6 particle layers showed no improvement. Although the highest G_{IC} values for PA6-d16a and PA6-d13r were observed when the particle areal weight was about 14 g/m^2, the values were almost the same as that of the non-toughened sample (0.24 kJ/m^2). The larger particle (PA6-d16a) seemed to provide a slightly higher G_{IC} than the smaller particle (PA6-d13r). However, the particle size did not influence the fracture toughness significantly.

4. Discussions

4.1 Particle amount vs. interlayer thickness

Interleaving particles increase the interlayer thickness. Figure 4 shows that the interlayer thickness is related to the particle size to some extent, as discussed in Section 3.1.

Figure 7a and 7b show the cross-sections of the DCB samples interleaved with PA6-d13r and PA12-d10s, respectively. Although the average size of those two particles is similar, the packing density of the smooth PA12-d10s particles was higher than the rough PA6-d13r particles at the interlaminar region. It was inferred that a greater size variation of the PA12-d10s particles (as shown in the SEM image in Table 1) contributed to increasing the particle packing density as the smaller particles can fill the gaps between the larger particles [29], which can be seen in the Figure 4a and 7b. For the PA6-d13r, particle layer thickness increased linearly with the particle areal weight (Figure 4b). This could be attributed to its rough surface and relatively uniform size preventing particle-particle movement, which results in a lower packing density (Figure 7a). In other words, including rough particles at the interlaminar region might lead to a lower bulk factor as the particle layer would become 'less compactable'. The lower bulk factor could be beneficial in such a case where less thickness reduction could minimise ply wrinkling when curing thick curved composite parts [30].

4.2 Particle amount vs. fibre volume fraction

As shown in Figure 8, the particle tougheners at the interlayers could increase the laminate thickness significantly, depending on their areal weight. This can affect the structural performance of the laminate.

By assuming that the nylon particles do not affect the modulus of the interlayer epoxy matrix due to its similar modulus and the fibre volume fraction of each fibre layer is constant, the in-plane tensile modulus of the unidirectional laminate can be easily calculated; the increased thickness of the interlayer and the fixed amount of the fibres result in reduction of the overall fibre volume fraction. Figure 9 shows the reduced tensile modulus at fibre direction calculated using the rule of mixture, for PA12-d10s particle as an example. The interlayer thickness used

in this calculation is from the data in Figure 4. The interlaminar fracture toughness is also plotted, which is from the data in Figure 6. As shown in Figure 9, although 10 g/m^2 of the particle areal weight approximately doubled the G_{IC}, the modulus is significantly decreased by 14.2%.

4.3 SEM observation

Laminates interleaved with nylon 6 and nylon 12 particles exhibited completely different fractured surface morphology, as shown in Figure 10 and Figure 11. With nylon 12 particles, the crack went through the particles causing fracture of the particles, as shown in Figure 10a. Due to the yielding, the particles effectively bridged the cracked surface preventing its rapid propagation. As shown in Figure 10b, the PA12-d10s particles were plastically deformed forming long tails at the centres of the particles before final fracture, which implies that strong particle-matrix bonding was formed as the curing temperature was close to or higher than the melting temperature of the nylon particles. Similar particle bridging was reported by Cardwell *et al*. [12] where the nylon 12 particles were used to toughen a neat epoxy resin. In their study, the curing temperature (120°C) was far below the melting point of particle, but the 16 hours long curing enabled the amine group to react with liquid resin before gelation.

However, particle bridging was not observed in the specimens toughened with the nylon 6 particles. As shown in Figure 11a, the crack path followed the particle-matrix interface, and crack deflection was the main role of the nylon 6 particles. The PA6-d16a particles were pulled out from the resin layer on the fractured surface (Figure 11b), which implies that the particle-matrix bonding strength was too weak to withstand the crack opening stress, causing no plastic deformation in the load-displacement curve (Figure 5d).

4.4 Toughening mechanism

The failure mechanism of the nylon 6 particle-toughened samples was similar to the case where impenetrable rigid particles are used as tougheners. Nakamura and Yamaguchi [31] investigated

the toughening effect of epoxy including silica particles. They concluded that the larger particles are more effective to impede crack propagation by diverting the crack tip along a longer path, leading to higher energy absorption, which could explain the slightly higher G_{IC} values of the samples toughened with PA6-d16a particles compared to those toughened with PA6-d13r particles. In contrast, in the nylon 12 particle toughened samples, most of the fracture energy was absorbed by the plastic deformation of the particles. Since the toughening effect was mainly dependent on the density of the particle bridging on the fractured surface, the smaller particles (PA12-d5s and PA12-d10s) resulted in higher G_{IC} values than the larger particles (PA12-d30a) at a similar particle areal weight, as shown in Figure 6b.

4.5 Effect of processing conditions

Although both nylon 6 and nylon 12 have similar chemical and mechanical properties (Table 1), their toughening effect was completely different depending on the processing condition. Based on the discussion in literature about the semi-IPN [17,18], it was deduced that the superior toughening effect of nylon 12 particle was due to its melting point close to the curing temperature of the prepreg resin matrix. In order to investigate the effect of the curing temperature in relation to the different melting points of the two nylon types, additional DCB test samples with different nylon 12 particle areal weights were manufactured using the same fabrication method but cured at 140°C for 5 hours, which was long enough to achieve approximately 75% of degree of cure [32].

In contrast with the load-displacement curve shown in Figure 5b, the test results showed there was no obvious ductile behaviour, as shown in the Figure 12a. In Figure 12b, the initiation G_{IC} had no relationship with the particle areal weight. As shown in Figure 13, the fractured surfaces were completely different between the specimens cured at 180°C (Figure 13a) and 140°C (Figure 13b). The sample cured at 140°C has a failure surface similar to the sample toughened

with nylon 6 particles, which showed particle-matrix debonding and particle pull-out (Figure 13b). The load-displacement curve in the DCB test (Figure 12a) also showed a similar response (Figure 5c), as no particle bridging occurred during the crack propagation. This result suggests that the curing temperature significantly changes the particle-matrix interfacial strength and influences the interlaminar toughing mechanism. Although this interfacial strength can be promoted with longer processing time at a lower temperature [12], this approach may not be cost-efficient in high volume production. Therefore, it is essential to choose a thermoplastic particle toughener that has a melting point close to or below the curing temperature of the prepreg matrix system.

5. Conclusion

In summary, this study focused on the effect of nylon particle characteristics on the interlaminar toughening effect. A range of different nylon 6 and 12 particles with different sizes and shapes was spread directly onto the surface of unidirectional carbon fibre/epoxy prepregs, and DCB specimens were manufactured to measure the interlaminar fracture toughness as well as the thickening effect.

It was found that the particle size and shape as well as the deposition amount affect the interlaminar toughness. However, the most important factor was the curing condition such as the difference between the curing temperature (180ºC) and the melting point of the particle, which determines the particle-matrix bonding strength. Well-established particle-matrix bonding in the nylon 12 toughened samples resulted in failure with significant plastic deformation of particles (particle bridging), which led to high initiation and propagation G_{IC}. In contrast, the failure in the nylon 6 particle-toughened samples occurred at the particle-matrix interface. The ductility of the particle and its better mechanical property than the nylon 12 were unable to contribute to fracture energy absorption. Consequently, the G_{IC} was very close to that of non-toughened samples, and the particles even negatively affected the in-plane mechanical property due to the thickening effect. The effect of the particle surface morphology on the

interfacial bonding strength was minimal, while it considerably affected the laminate thickening.

The importance of interfacial bonding strength in toughening was further demonstrated by applying a lower curing temperature (140ºC) to the samples toughened with the nylon 12 particles. The G_{IC} was significantly reduced, and no obvious ductile response was observed in the load-displacement curve. SEM images revealed that the dominant failure mechanism was particle-matrix debonding and particle pull-out, which was similar to that of the nylon 6 toughened samples.

When sufficient interfacial bonding can be achieved, smaller particles were more effective, which appeared to be related to the increased density of particle bridging. In the range of particle areal weight used in this work (5 - 35g/m^2), more nylon 12 particles resulted in higher G_{IC}. However, its impact on other mechanical properties such as in-plane mechanical properties due to the reduced fibre volume needs to be considered.

If a commercial prepreg with a particle toughened resin system is used, it is difficult to achieve both high in-plane modulus/strength and high interlaminar toughness (or damage tolerance) at the same time due to the thickening effect. Direct particle deposition method used in this work has a great advantage in that the particle tougheners can be selectively applied only to the areas requiring high delamination resistance. Furthermore, the method could be implemented in an automated fibre or tape deposition process to produce toughened prepreg tapes on the fly. It could also allow for converting a prepreg product with low toughness into a highly toughened product in a cost-effective way.

Acknowledgements

This work was supported by the Engineering and Physical Sciences Research Council through the EPSRC Centre for Doctoral Training in Advanced Composites for Innovation and Science

[grant number EP/L016028/1]. We thank the Polyamide Polymers Department of Toray Industries in Japan who provided the materials for this work. All data required for reproducibility are provided within the paper.

Reference

[1] Sultan JN, McGarry FJ. Effect of rubber particle size on deformation mechanisms in glassy epoxy. Poly Eng Sci 1973;13:29–34. doi:10.1002/pen.760130105.

[2] Garg AC, Mai YW. Failure mechanisms in toughened epoxy resins-A review. Compos Sci Technol 1988;31:179–223. doi:10.1016/0266-3538(88)90009-7.

[3] Kim JK, Robertson RE. Toughening of thermoset polymers by rigid crystalline particles. J Materials Sci 1992;27:161–74. doi:10.1007/BF00553852.

[4] Pearson RA, Yee AF. Toughening mechanisms in thermoplastic-modified epoxies: 1. Modification using poly(phenylene oxide). Polym 1993;34:3658–70. doi:10.1016/0032-3861(93)90051-B.

[5] Pearson RA. Toughening Epoxies Using Rigid Thermoplastic Particles. In: Riew CK, Kinloch AJ, editors. Toughened Plastics I 1993;233:405–25. doi:10.1021/ba-1993-0233.ch017.

[6] Bascom WD, Cottington RL, Jones RL, Peyser P. The fracture of epoxy- and elastomer-modified epoxy polymers in bulk and as adhesives. J App Polym Sci 1975;19:2545–62. doi:10.1002/app.1975.070190917.

[7] Sela N, Ishai O, Banks-Sills L. The effect of adhesive thickness on interlaminar fracture toughness of interleaved cfrp specimens. Composites 1989;20:257–64. doi:10.1016/0010-4361(89)90341-8.

[8] Ishai O, Rosenthal H, Sela N, Drukker E. Effect of selective adhesive interleaving on interlaminar fracture toughness of graphite/epoxy composite laminates. Composites 1988;19:49–54. doi:10.1016/0010-4361(88)90543-5.

[9] Davies P, Kausch HH, Williams JG, Kinloch AJ, Charalambides MN, Pavan A, Moore DR, Prediger R, Robinson I, Burgoyne N, Friedrich K, Wittich H, Rebelo CA, Torres Marques A, Ramsteiner F, Melve B, Fischer M, Roux N, Martin D, Czarnocki P. Round-robin interlaminar fracture testing of carbon-fibre-reinforced epoxy and PEEK. Composites Science and Technology 1992;43:129–36. doi:10.1016/0266-3538(92)90003-L

[10] Tahir MW. Dual Scale Porosity and Interlaminar Properties of Composite Materials. KTH Royal Institute of Technology in Stockholm, 2014

[11] Faber KT, Evans AG. Crack deflection processes-I. Theory. Acta Metall 1983;31:565–76. doi:10.1016/0001-6160(83)90046-9.

[12] Cardwell BJ, Yee AF. Toughening of epoxies through thermoplastic crack bridging. J Mater Sci 1998;33:5473–84. doi:10.1023/a:1004427123388.

[13] Gawin I, Swetlin BJ. Damage tolerant composites containing infusible particles. Compos Manuf 2008;1:265. doi:10.1016/0956-7143(90)90081-7.

[14] Maranci A, Peake SL, Kaminski SS. Advance composites with thermoplastic particles an the interface between layers. US 4957801, 1990.

[15] Paris C. Etude et Modélisation de la Polymérisation Dynamique de Composites à Matrice Thermodurcissable. Universite of Toulouse, 2011.

[16] Kishi H, Uesawa K, Matsuda S, Murakami A. Adhesive strength and mechanisms of epoxy resins toughened with pre-formed thermoplastic polymer particles. J Adhes Sci Technol 2005;19:1277–90. doi:10.1163/156856105774784402.

[17] Nichols ME, Robertson RE. The toughness of epoxy-poly(butylene terephthalate) blends. J Mater Sci 1994;29:5916–26. doi:10.1007/BF00366876.

[18] Kim S, Kim J, Lim SH, Jo WH, Choe CR. Effects of mixing temperatures on the morphology and toughness of epoxy/polyamide blends. J App Polym Sci 1999;72:1055–63. doi:10.1002/(SICI)1097-4628(19990523)72:8<1055::AID-APP10>3.0.CO;2-8.

[19] Park BY, Kim SC, Jung B. Interlaminar Fracture Toughness of Carbon Fiber / Epoxy Composites using Short Kevlar Fiber and/or Nylon-6 Powder Reinforcement. Polym Advan Technol 1997;8:371–7. doi:10.1002/(SICI)1099-1581(199706)8:6<371::AID-PAT658>3.0.CO;2-I.

[20] Hunt C, Kratz J, Partridge IK. Cure path dependency of mode I fracture toughness in thermoplastic particle interleaf toughened prepreg laminates. Composites Part A-Appl S 2016;87:109–14. doi:10.1016/j.compositesa.2016.04.016.

[21] Gilbert EN, Hayes BS, Seferis JC. Interlayer toughened unidirectional carbon prepreg systems: Effect of preformed particle morphology. Composites Part A-Appl Sci 2003;34:245–52. doi:10.1016/S1359-835X(02)00141-0.

[22] Gao F, Jiao G, Lu Z, Ning R. Mode II Delamination and Damage Resistance of Carbon/Epoxy Composite Laminates Interleaved with Thermoplastic Particles. J Compos Mater 2007;41:111–23. doi:10.1177/0021998306063356.

[23] Yasaee M, Bond IP, Trask RS, Greenhalgh ES. Mode I interfacial toughening through discontinuous interleaves for damage suppression and control. Composites Part A-Appl Sci 2012;43:198–207. doi:10.1016/j.compositesa.2011.10.009.

[24] WangY-S, WuY-J. Epoxy resins with improved burn properties. US 8039109, 2011.

[25] Hexcel. HexPly® 8552 Epoxy Matrix - Product Data Sheet. https://www.hexcel.com/Resources/DataSheets/Prepreg

[26] D5528 - Standard Test Method for Mode I Interlaminar Fracture Toughness of Unidirectional. ASTM Stantards 2006;03:1–15. doi:10.1520/D5528-01R07E03.2.

[27] HexTow ® IM7 Carbon Fiber - Product Data Sheet. https://www.hexcel.com/Resources/DataSheets/Carbon-Fiber

[28] Hexcel. HexPly ® M21 - Product Data Sheet. https://www.hexcel.com/Resources/DataSheets/Prepreg

[29] Sohn HY, Moreland C. The effect of particle size distribution on packing density. The Can J Chem Eng 1968;46:162–7. doi:10.1002/cjce.5450460305.

[30] Belnoue JP-H, Nixon-Pearson OJ, Thompson AJ, Ivanov DS, Potter KD, Hallett SR. Consolidation-Driven Defect Generation in Thick Composite Parts. J Manuf Sci Eng 2018;140:071006. doi:10.1115/1.4039555.

[31] Nakamura Y, Yamaguchi M, Okubo M, Matsumoto T. Effect of particle size on the fracture toughness of epoxy resin filled with spherical silica. Polymer 1992;33:3415–26. doi:10.1016/0032-3861(92)91099-N.

[32] Clarkson E. Hexcel 8552 IM7 Unidirectional Prepreg 190 gsm & 35 % RC Qualification Statistical Analysis Report. NCP-RP-2009-028, Wichita State University: 2011.

Figures

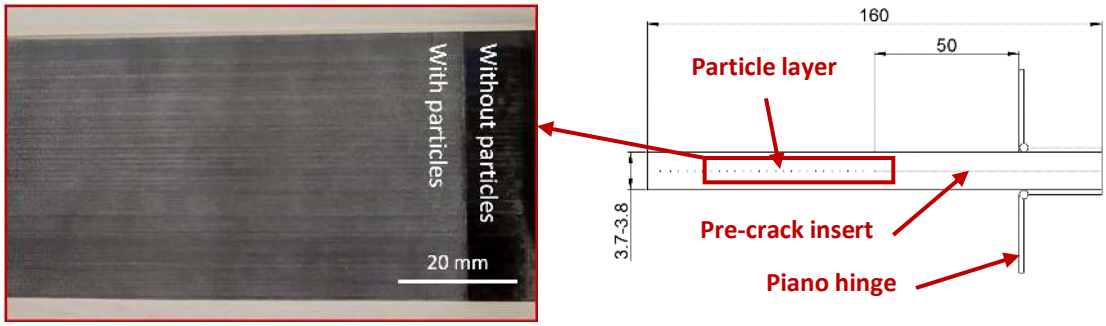

Particle layer (PA12-d30a, ~5.2 g/m^2) on prepreg surface

Figure 1 Schematic of the manufacturing method for the DCB test samples with a photo of the prepreg surface coated with particles (dimensions in mm).

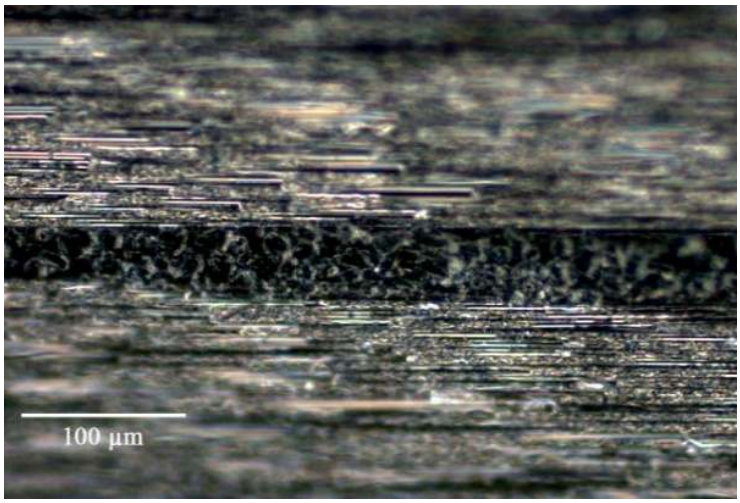

Figure 2 Microscopic image of the cross-section of the particle toughened interlayer for thickness measurement (PA6-d16a, 27.8 g/m^2).

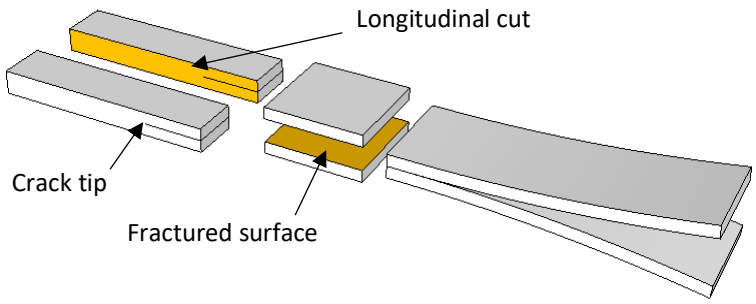

Figure 3 Illustration of the observed surfaces (yellow) from the cut sample using SEM.

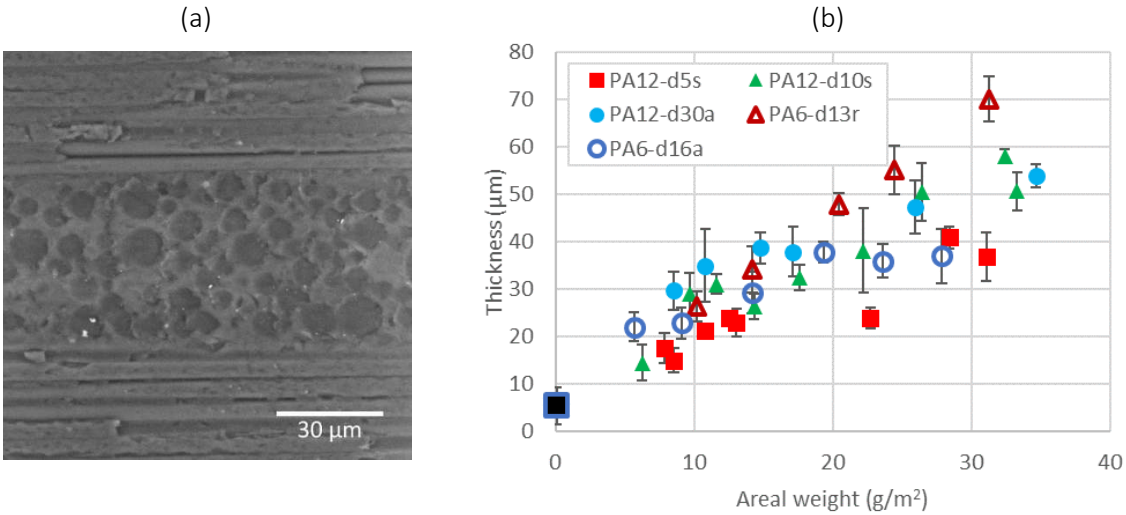

Figure 4 Interlaminar resin layer including the particle tougheners: (a) SEM image of PA12-d10s (32 g/m^2) toughened interlayer, (b) Interlayer thickness change of the DCB samples interleaved with different nylon particles.

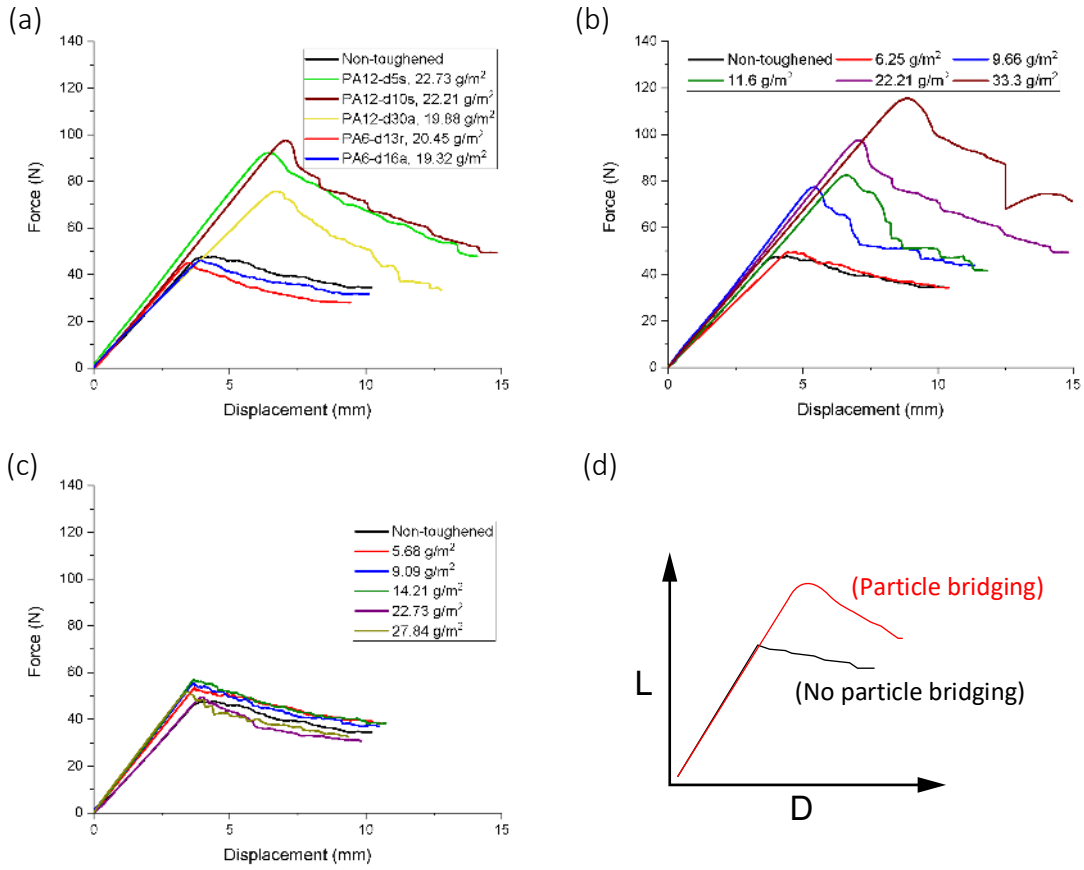

Figure 5 Load-displacement curves in the DCB tests of the samples interleaved with: (a) different particles with areal weights close to 20 g/m^2, (b) PA12-d10s, (c) PA6-d16a, and (d) typical load-displacement response between with and without particle bridging.

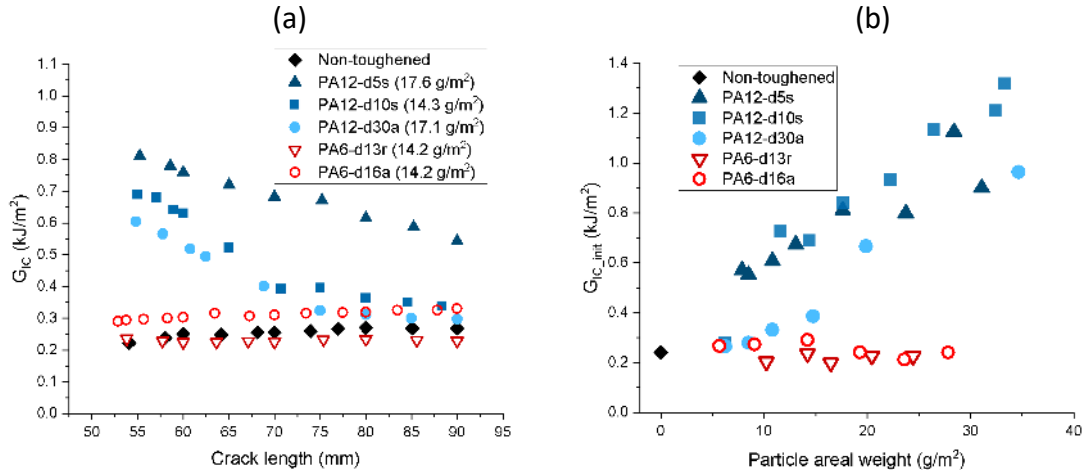

Figure 6 R-curves and initiation G_{IC} values: (a) The R-curves of the samples interleaved with different nylon particles (particle areal weight: approximate 15 g/m^2), (b) the initiation G_{IC} of the samples interleaved with different areal weight of nylon particles.

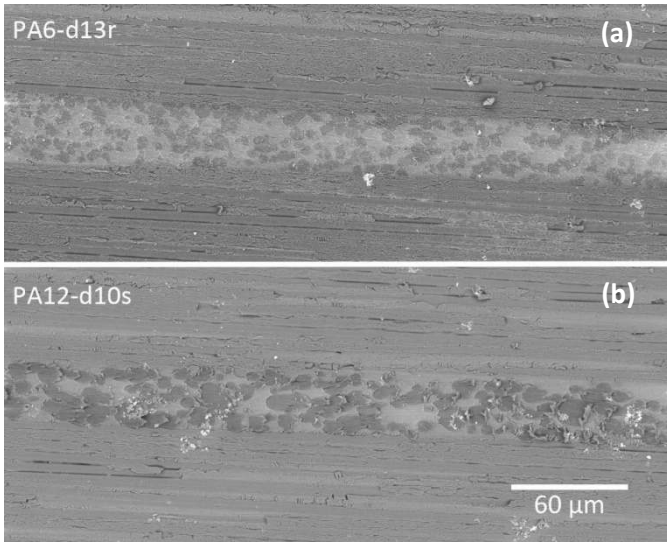

Figure 7 SEM images of the cross-section of the laminates interleaved with (a) PA6-d13r (16.5 g/m^2) and (b) PA12-d10s (17.6 g/m^2) particles.

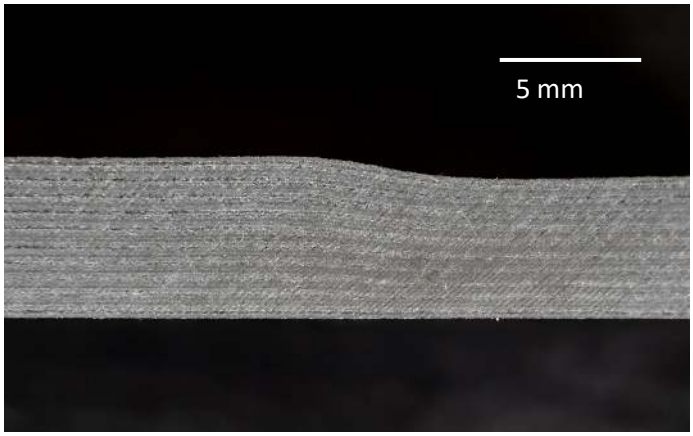

Figure 8 Cross-section view of a cured IM7/8552 laminate made of 40 plies (left: all interlayers interleaved with PA12-d30a particles at 9 g/m^2, right: without particles).

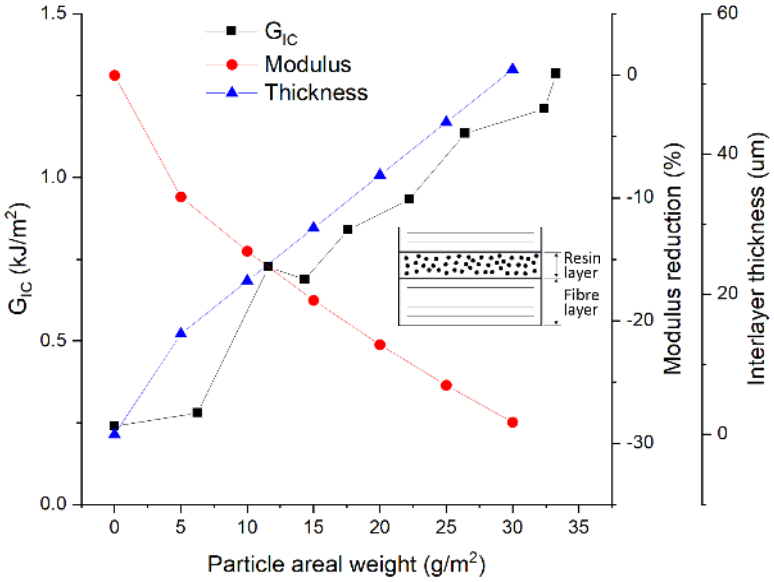

Figure 9 Effect of the PA12-d10s particle amount on the in-plane tensile modulus, G_{IC} and the interlayer thickness of a unidirectional IM7/8552 laminated composite.

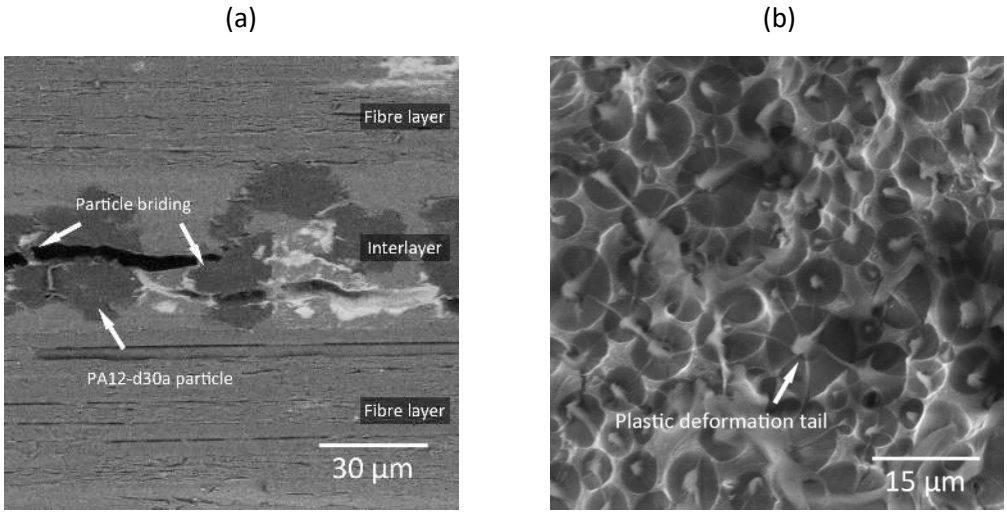

Figure 10 SEM images of nylon 12 toughened samples: (a) side view of sample toughened with PA12-d30a and (b) fractured surface of the sample toughened with PA12-d10s.

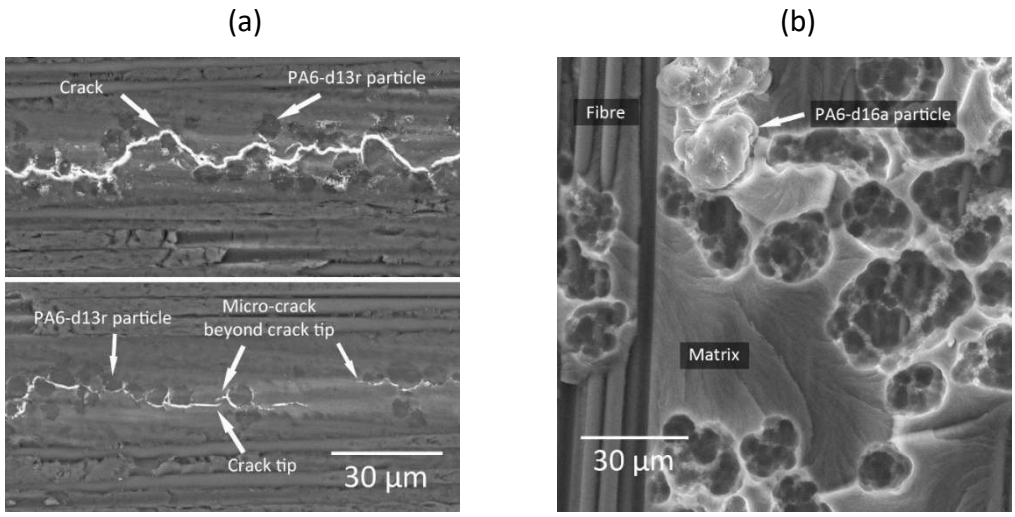

Figure 11 SEM images of nylon 6 toughened samples: (a) side views of the sample toughened with PA6-d13r (top: the crack path after the propagation, bottom: the area near the crack front) and (b) fractured surface of the sample toughened with PA6-d16a.

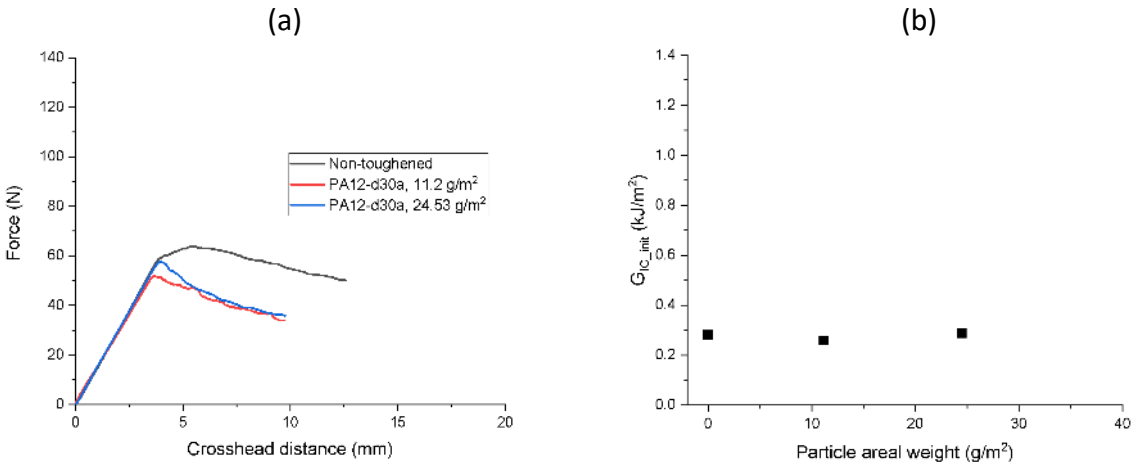

Figure 12 DCB test results of the sample interleaved with PA12-d30a cured at 140°C for 5 hours: (a) load-displacement curve and (b) initiation G_{IC} values for different particle areal weights.

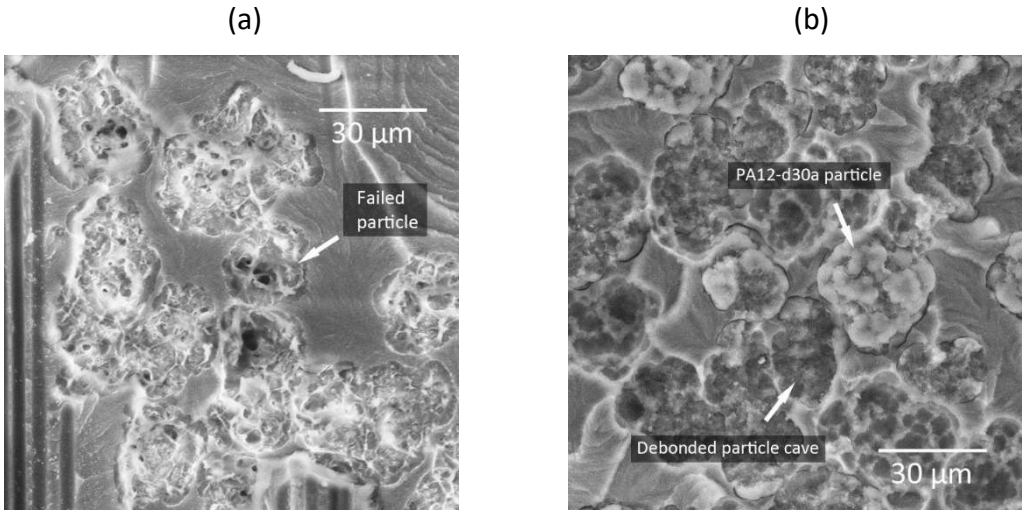

Figure 13 SEM images of the fractured surfaces of the DCB samples that were toughened with PA12-d30a and cured at: (a) 180°C and (b) 140°C.